Journal of Alloys and Compounds 480 (2009) 878–881

Contents lists available at ScienceDirect

Journal of Alloys and Compounds

journal homepage: www.elsevier.com/locate/jallcom

Plasmon loss and valence band structure of silicon-based alloys deposited by hot wire chemical vapor deposition

Bibhu P. Swain*, Bhabani S. Swain, Sung H. Park, Nong M. Hwang

National Research Laboratory of Charged Nanoparticles, Department of Materials Science and Engineering, Seoul National University, Seoul, South Korea

ARTICLE INFO

Article history:
Received 14 October 2008
Received in revised form 15 February 2009
Accepted 18 February 2009
Available online 3 March 2009

Keywords:
Silicon-based alloys
HWCVD
XPS

ABSTRACT

Silicon-based alloys have been deposited by hot wire chemical vapor deposition (HWCVD). For nc-Si:H films $SiH_4 + H_2$ gas mixture have been used, whereas for a-SiC:H and a-SiN:H films $SiH_4 + CH_4 + H_2$ and $SiH_4 + NH_3 + H_2$ gas mixtures have been employed. We observed a plasmon loss peak for amorphous films and two peaks for nc-Si embedded silicon alloy films. The total plasmon loss peak is the contribution of 18–26% of from main Si(2p) core orbital. The FWHM of valence band of alloy increases with increase of carbon and nitrogen content.

1. Introduction

Amorphous silicon-based films deposited by hot wire chemical vapor deposition (HWCVD) technique have been intensively investigated, due to their application in electronic devices such as thin film transistors, solar cells, light emitting devices, color sensors, quantum well structures [1,2]. However, till now very few papers have analyzed the analogies and differences between silicon-carbon and silicon nitrogen alloys, taking also into account the possibility to deposit materials having similar physical properties [3,4]. On the contrary, a complete understanding of analogies and differences in electronic properties of the two alloys are necessary for a more efficient use in electronic devices. Aim of this study is to give for the first time a comparative picture of valence band of high electronic quality a-SiC:H and a-SiN:H films in the HWCVD system. Moreover, the a-SiC:H and a-SiN:H alloys, which are known to have a more complex structure for the presence of carbon and nitrogen, respectively [5–7], has been deposited with different carbon sources and the a-SiN:H alloy has been deposited in standard silane-ammonia precursor gas [8]. Plasmon loss energy is strongly correlated with mechanical and structural properties of amorphous and nc-silicon embedded in amorphous films. Plasmons are collective longitudinal excitations of the outer electrons in a solid [9]. In the free electron approximation, the relation between the plasmon energy $h\omega_p$ of a Drude gas of electrons with volume density n_v is given as

$$\omega_p = \left(\frac{n_v e^2}{\varepsilon_0 m}\right)^{1/2}, \quad (1)$$

where e is the electron charge, m is the electron mass and ε_0 is the permittivity of free space. However they also appear as distinctive satellite peaks at high binding energy (BE) near core lines in photoelectron spectra. The valence electrons in the semiconductor and insulator materials undergo collective oscillation provided the plasma energy is much greater than the band gap. The straightforward approach to inclusion of the effect of the band gap E_g is based on the assumption that the oscillator strength for interband excitations is given as [10]:

$$\omega_p = \left(\frac{n_v e^2}{\varepsilon_0 m} + E_g^2\right)^{1/2} \quad (2)$$

In the present article, we focus on the core orbital of Si(2p), with carbon and nitrogen alloying elements and their plasmon loss for nc-Si embedded amorphous alloys. The valence band of constitutive alloys in the silicon matrix is also discussed.

2. Experimental

Amorphous silicon and its alloys were prepared by hot wire chemical vapour deposition by using SiH_4, CH_4, NH_3 and H_2, precursors on corning glass (7059) and Si wafer. Deposition of amorphous silicon (a-Si:H) and nanocrystalline silicon (nc-Si) were done by using SiH_4 and H_2 precursors. Hydrogenated amorphous silicon carbon (a-SiC:H), silicon nitride (a-SiN:H) alloys were deposited by using $SiH_4 + CH_4 + H_2$ and $SiH_4 + SiN_3 + H_2$ precursors. The detail deposition parameters of silicon and silicon-based alloys are listed in Table 1. XPS analysis was performed

* Corresponding author. Present address: Research Center for Photovoltaics, National Institute of Advanced Industrial Science and Technology, AIST-2 Umezono 1-1-1, Tsukuba, Ibaraki 305-8568, Japan. Tel.: +82 28809152; fax: +82 2889152.
E-mail addresses: bp.swain@aist.go.jp, bibhuprasad.swain@gmail.com (B.P. Swain).

0925-8388/$ – see front matter © 2009 Elsevier B.V. All rights reserved.
doi:10.1016/j.jallcom.2009.02.057

Table 1
Deposition parameters for silicon-based alloys films.

Precursor gases silicon films	SiH_4 = 1 sccm (60% H_2) H_2 = 5–25 sccm
Precursor gases for SiC films	SiH_4 = 1 sccm (60% H_2) CH_4 = 0.1, 0.2, 0.3, 0.4 and 0.5 H_2 = 10 sccm
Precursor gas for SiN films	SiH_4 = 1 sccm NH_3 = 0.1, 0.2, 0.3, 0.4 and 0.5 H_2 = 10 sccm
Process pressure	500 mTorr
Substrate temperature	200 °C
Filament temperature	1800 °C

on the as-deposited films using a VG ESCA-LABMK II system equipped with a non-monochromatic Mg Kα X-ray (1253.6 eV) source, with a residual pressure of 10^{-10} Torr. The electron spectrometer was calibrated by assuming that the binding energy of the Au $4f_{7/2}$ line is 83.9 eV with respect to the Fermi level. The uniformity of the composition was confirmed over the entire area of the substrate. In order to remove the native oxide on the surface the samples were immersed in 2% HF solution for 2 min before the measurements and the contribution due to physically absorbed carbon was removed in the decomposition by Ar+ etching.

3. Result and discussions

Fig. 1(a–c) shows Si(2p) core orbital spectra of a-Si:H, a-SiN:H and a-SiC:H films deposited by HWCVD. The peak positions of a-Si:H, a-SiC:H and a-SiN:H are found at 98.6 eV, 99.2 eV and 100.5 eV, respectively. After deconvolution of Si(2p) into two peaks, Si–Si and Si–H bondings appear at 98.52 eV and 99.25 eV, respectively, in a-Si:H film. Though the hydrogen content cannot be detected in XPS measurement, Si(2p) core orbital has an asymmetric nature and shifts to higher energy due to electronegative difference between Si and H. In Fig. 1(b and c), Si–Si and Si–N peaks appear at 100.3 eV and 100.9 eV, respectively, for a-SiN:H and Si–Si and Si–C core orbital peaks appear at 99.08 eV and 100.8 eV, respectively, in a-SiC:H films. The shifts of Si(2p) core orbital peaks are due to involvement of higher electronegative atoms [5–7].

Fig. 2(a–c) shows the plasmon loss of silicon and silicon-based alloys. It illustrated two series of plasmon peaks: (a) ones from amorphous network and (b) the others from nc-Si embedded with Si–H, Si–C and Si–N matrices. The intensity of plasmon loss depends on density of materials and the volume of plasmon is directly related to the dielectric function of the medium. The contents with a single broad one are observed for pure amorphous networks. The details of the plasmon losses are as follows: (a) ~17 eV peak is due to the Si bulk plasmon [11], coming from the core of the nc-Si and (b) 30–40 eV plasmon losses is attributed to nc-Si embedded SiC, SiN and SiH matrix. The plasmon loss peak appears at ~23 eV is due to the surrounding in a-SiC:H and a-SiN:H networks, forming a pure amorphous network [6]. The total plasmon loss peak is the contribution of 18–26% from a main Si(2p) core orbital. The energy of surface plasmon appears at lower to bulk plasmon of the nc-Si. The minor features at 5.5–6 eV correspond to the inter-band transition due to alloying with carbon, oxygen and nitrogen [12].

Investigating the valence band of the a-Si:H, a-SiC:H and a-SiN:H films containing nc-Si, we find large differences due to the presence of the silicon clusters. Fig. 3 shows how the valence band structures of nc-Si:H vary with a H_2 flow rate varying from 5 sccm to 25 sccm. Hennig et al. reported the details about the valence band structure of amorphous silicon by the density-matrix functional method [13]. This indicates three major structures A, B, and C which correspond, respectively, to 2p like silicon bonding states between 2.5 eV and 10 eV and to a mixture of Si(3s) and Si(2p) bonding states between 10 eV and 15 eV. The Si(2s) like peak is observed from 15 eV to 25 eV. The transition of s orbital from C region at 25 eV shifts to D or E

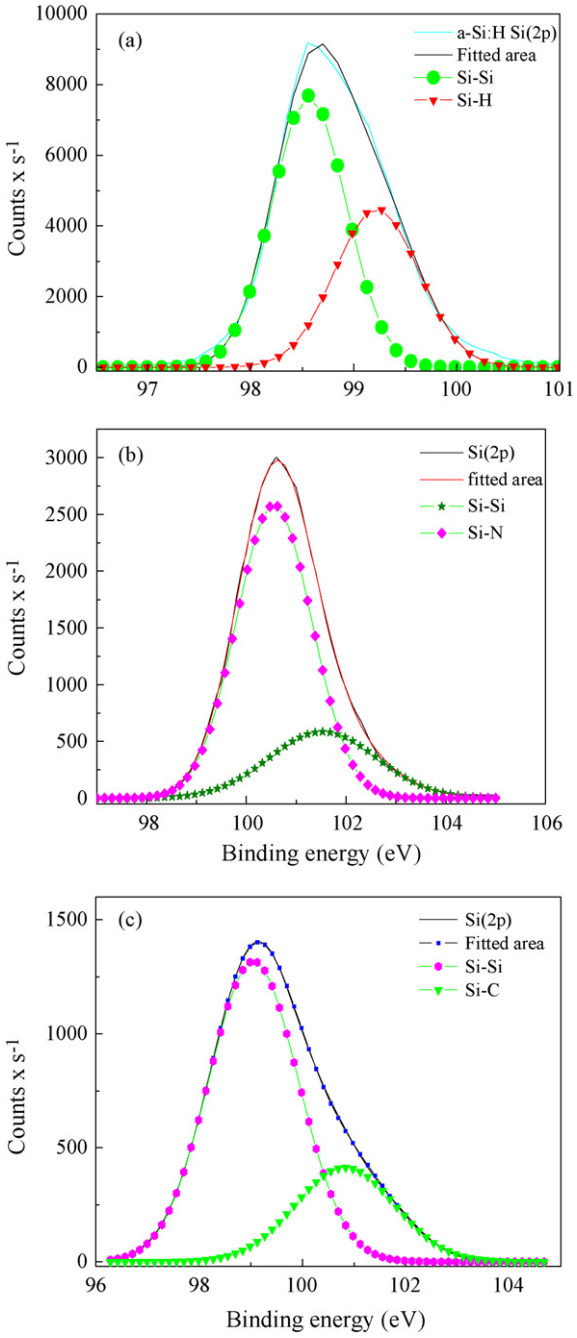

Fig. 1. Core Si(2p) spectra (a) Si:H, (b) SiN, and (c) SiC film.

region at the lower energy of 21–22 eV, indicating the structural change from amorphous silicon to nc-Si and microcrystalline silicon. The ionic characters of Si–H bond and the inhomogenity in a-Si:H films shows the appearance of Si–Si and Si–H bonds which reflects increase in the broadness of the valence and overlapping of orbital in a-Si:H films.

Fig. 4 shows that valence band structure of a-SiC:H and nc-Si embedded a-SiC:H films with a CH_4 flow rate varying from 0.1 sccm to 0.5 sccm. With CH_4 at 0.1 sccm, the film appears to be nc-Si embedded a-SiC:H film while it is a pure amorphous film with CH_4 at 0.3 sccm. 0–2.5 eV represents unbounded atoms present at the mid-gap states of a-SiC:H films and the densities of states increase with CH_4 flow rates. If we compare the theoretical valence band structure of a-SiC:H alloys, it would be instructive to compare their valence band spectra with that of the 2H-SiC sample and the cal-

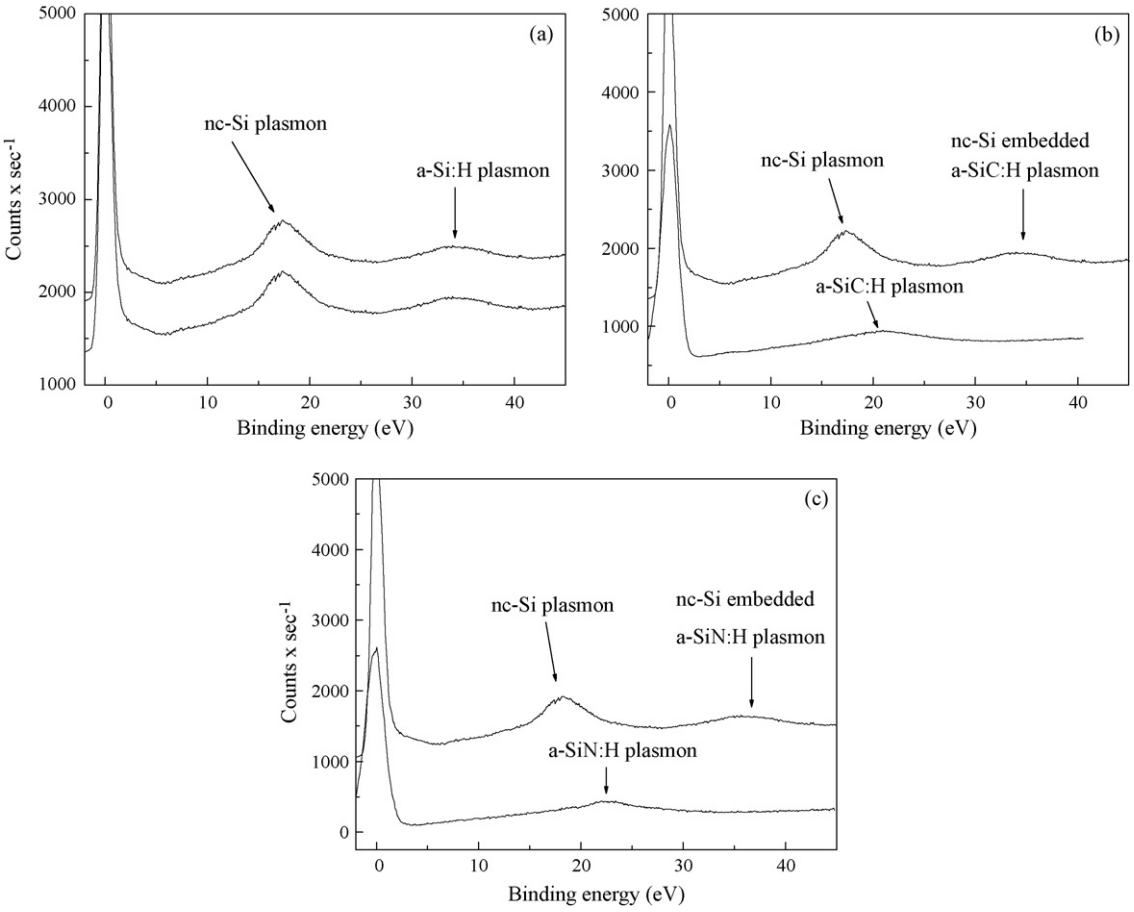

Fig. 2. Plasmon loss peak of nc-Si embedded a-Si:H films (a), plasmon loss peak of a-SiC:H and nc-Si embedded a-SiC:H films (b) and plasmon loss peak of a-SiN:H and nc-Si embedded with a-SiN:H films (c).

culated density of states (DOS) for the cubic (zinc-blende) β-SiC modification due to Robertson [14,15]. Both structures consist of a tetragonal arrangement of Si and C atoms and the only difference is the relative orientation of neighboring tetragonal along a connecting bond: staggered for the cubic or zinc blend and eclipsed for the hexagonal or wurtzite structure. Fig. 4 indicates three major structures A, B, C and D, which corresponds, respectively, to Si(3p)–C(2p) lone pair bonding states between 2.5 eV and 7 eV and a mixture of Si(3s) and Si(3p) and C(2s) bonding states between 7 eV and 15 eV. The s like peak observed from 15 eV to 20 eV is assigned to the region of E and F. The ionic character of Si–C bond and the inhomogenity in a-SiC:H films shows the appearance of Si–Si and C–C bonds which

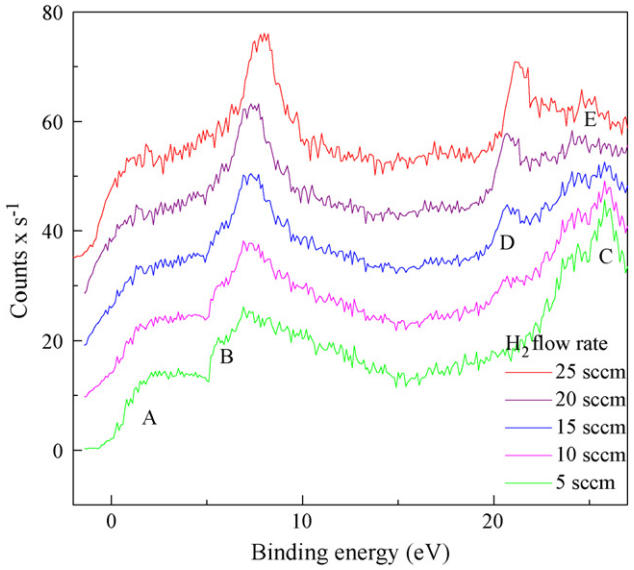

Fig. 3. Valence band of nc-Si:H with varying H_2 flow rate.

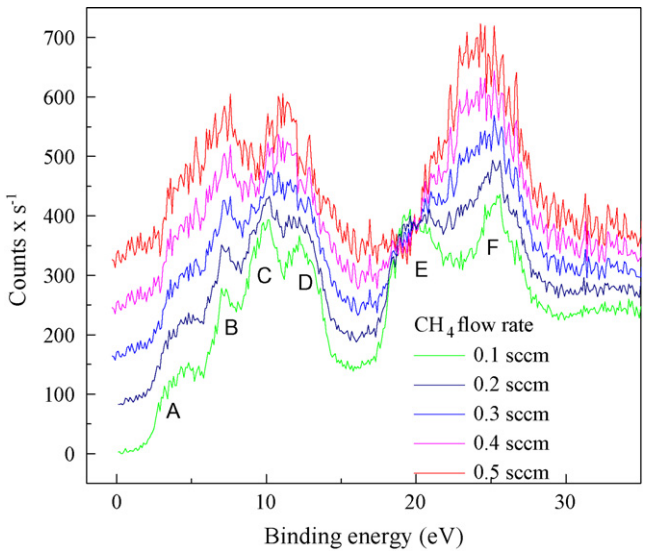

Fig. 4. Valence band of a-SiC:H and nc-Si embedded with a-SiC:H with varying CH_4 flow rate.

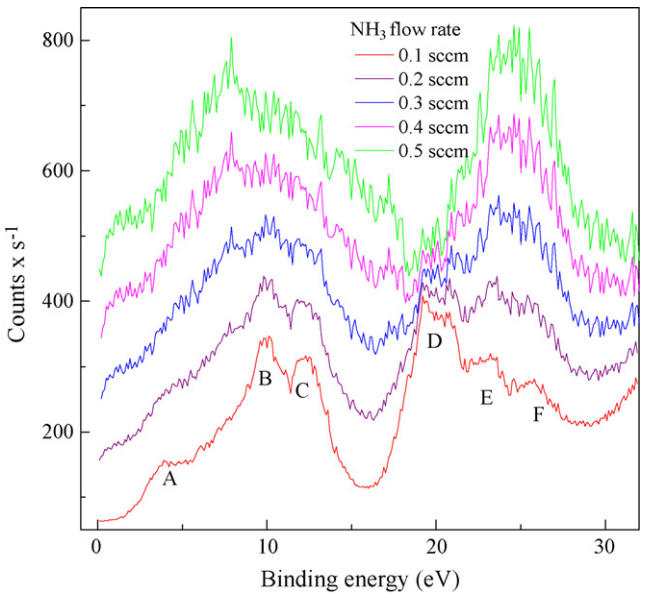

Fig. 5. Valence band of a-SiN:H and nc-Si embedded a-SiN:H with varying NH_3 flow rate.

reflects the increase in the broadness of the valence and overlapping of orbital in a-SiC:H films [16–18].

Fig. 5 shows the variation of the valence band structure of a-SiN:H and nc-Si embedded a-SiN:H films with a NH_3 flow rate varying from 0.1 sccm to 0.5 sccm. The valence band is more distinguished for a NH_3 flow rate of 0.1 sccm, confirming the presence of nc-Si in a-SiN:H films. The valence band orbitals are overlapping each other and a higher NH_3 flow rate approaches films, which are purely amorphous. Valence bands of nc-Si(N:H) and a-SiN:H films can be classified into six regions. Nanocrystalline silicon embedded a-SiN:H films are at 0.1 sccm NH_3 flow rate, while increasing NH_3 flow rate decreases the nc-Si contribution. Films prepared at 0.3–0.5 sccm NH_3 flow rate are purely amorphous. The 0–5 eV (A region) is characterized for non-bonded dangling bonds attributed to the replacement of a nitrogen loan pair by Si(3p)–Si(3p) states. The region 7.5–12 eV is attributed to p-like valence band, while 12.5–15 eV region is sp like. More confined features from A to F are characteristics of SiN and attributed to the valence peaks Si(2p) and N(2p) lone pairs, Si(3s)–N(2p), Si(3p)–N(2p) orbital, N(2s) and O(2s), respectively. Karcher et al. reported the similar results in a-SiC:H films [19]. The individual orbitals are more distinguishable in a crystalline nanostructure while they are wider monotonically with nitrogen incorporation. It can be noticed that the N(2s) band of the N-rich sample E and F is more broadened at the top of the peak, indicating the presence of various chemical environments of nitrogen atoms. The valence band of nc-Si(N:H) films exhibits a feature rebelled, which is probable due to Si–H chemical bonds according to data reported by other authors [20–23]. It is attributed to Si(3p) electrons hybridized with H(1s) electrons. This experimental observation supports the increases of the optical band gap due to nitrogen incorporation in the film.

4. Conclusion

The valence band and plasmon loss characterization of amorphous and nc-Si embedded amorphous silicon films provided a series of interesting points as to their electronic features. The results obtained in the present study lead to the following conclusions; (a) a single plasmon loss peak is for amorphous films and two peaks for nc-Si embedded silicon are for alloys films, (b) the 2p and sp orbitals are overlapped each other and FWHM of the valence band is broader for both SiC and SiN films, increasing with carbon and nitrogen incorporation.

Acknowledgements

The authors acknowledge the financial support by the BK21 program and by the Korea Science and Engineering Foundation (KOSEF) through the National Research Laboratory program under project No. M10600000159-06J0000-15910.

References

[1] J. Rath, B. Stannowski, A.T.V.V. Patrick, K.V.V. Marieke, R.E.I. Schropp, Thin Solid Films 395 (2001) 320.
[2] S.B. Patil, A.A. Kumbhar, S. Saraswat, R.O. Dusane, Thin Solid Films 430 (2003) 257.
[3] G.H. Bauer, H.-D. Mohring, G. Bilger, A. Eicke, J. Non-Cryst. Solids 77–78 (1985) 873.
[4] T. Stapinski, G. Ambrosone, U. Coscia, F. Giorgis, C.F. Pirri, Physica B 254 (1998) 99.
[5] B.P. Swain, R.O. Dusane, Mater. Chem. Phys. 99 (2006) 240.
[6] B.P. Swain, Appl. Surf. Sci. 253 (2007) 8695.
[7] B.P. Swain, Surf. Coat. Technol. 201 (2006) 1589.
[8] B.P. Swain, B.S. Swain, N.M. Hwang, Appl. Surf. Sci. 255 (2008) 2557.
[9] C. Kittel, Introduction to Solid State Physics, 7th ed., Wiley, New York, 1996; H. Raether, Excitation of Plasmons, Springer, Berlin, 1980.
[10] I. Egri, Solid State Commun. 44 (1982) 563.
[11] M. Mitome, Y. Yamazaki, H. Takagi, T. Nakagiri, J. Appl. Phys. 72 (1992) 812.
[12] D. Ugarte, C. Colleix, P. Trebbia, Phys. Rev. B 45 (1992) 4332.
[13] R.G. Hennig, P.A. Fedders, A.E. Carlsson, Phys. Rev. B 66 (2002) 195213.
[14] J. Robertson, Adv. Phys. 35 (1986) 317.
[15] J. Robertson, E.O. Reilly, Phys. Rev. B 35 (1987) 2946.
[16] A. Santoni, J. Lancok, V.R. Dhanak, S. Loreti, G. Miller, C. Minarini, Appl. Phys. A 81 (2005) 991.
[17] N. Laidani, G. Speranza, L. Calliari, V. Micheli, M. Anderle, Surf. Coat. Technol. 151/152 (2002) 138.
[18] P. Melinon, P. Keghelian, A. Perez, C. Rey, J. Lenne, M. Pellarin, M. Broyer, M. Boudeulle, B. Champagnon, J.L. Rousset, Phys. Rev. B 58 (1998) 16481.
[19] R. Karcher, L. Ley, R.L. Johnson, Phys. Rev. B 30 (1984) 1896.
[20] Y. Katayama, T. Simada, T. Uda, K.L.I. Kobayashi, J. Non-Cryst. Solids 59/60 (1983) 561.
[21] L. Yang, B. Abeles, W. Eberthardt, D. Sonderricker, IEEE Trans. Elec. Dev. 36 (1989) 2798.
[22] P. Hammer, N.M. Victoria, F. Alvarez, J. Vac. Sci. Technol. A 16 (1998) 2941.
[23] G. Dupont, H. Caquineau, B. Despax, R. Berjoan, A. Dollet, J. Phys. D 30 (1997) 1064.